Chiral Silica

DOI: 10.1002/anie.201108914

# High-Temperature-Resistant Chiral Silica Generated on Chiral Crystalline Templates at Neutral pH and Ambient Conditions**

*Hiroyuki Matsukizono and Ren-Hua Jin**

*In memory of Tadatomi Nishikubo*

Chirality is one of the fundamental issues in the related fields of biology, medicine, chemistry, and physics,[1] because components of life, medicine, and display devices are composed of chiral molecules, such as DNA, proteins, cellulose, sugar, amino acids, drugs, and liquid crystalline molecules. However, chirality is not restricted to these molecular regimes. Solid minerals and inorganic materials also have chirality, which arises from the geometric properties and the atomic structure of surfaces.[1–3] A difference between molecular and mineral chirality would be in its resilience; the former is temporary at the limited environment, while the latter will be semi-permanent even under the harsh conditions. Therefore, artificial chiral minerals would have great potential for memory, preservation, and development of organic chiral systems.

Helical mesoporous silica, which was pioneered by Tatsumi et al,[4] is one of current topics in chiral mineral materials. Its chirality is induced by a templated sol–gel reaction where special micelles self-assembled from chiral molecules serve as templates to direct helical morphology, thereby imprinting the chiral topology in silica.[4,5] Although this is a refined process to simultaneously control the morphology and chirality, in conventional chiral mesoporous silica formation, the hydrolytic condensation of alkoxysilane is catalyzed by the added HCl or NaOH solution rather than by micellar template itself.[6–9] In the design of silica materials, the greatest designer and authority is surely biosilica, such as diatoms and sponges, which have very beautiful, complex, and sophisticated shapes in nano- and microdimensions with silica skeletons.[10–13] In this sense, diatoms and sponges are eternal texts with a lot of sources of inspiration for the synthesis of silica-based nano/microscale materials, including chiral silica. It is well known that in the biogenic silica formation, organized organic matrices, such as silaffins (polypeptides), silicateins (proteins), and long-chain polyamines play as catalysts (temporal control) and templates (spatial control) in silica deposition under neutral pH and ambient conditions.[14–24] As mimicking those organic matrices, a lot of organic molecules and polymers having amino groups have been used in the biomimetic silica deposition, and major achievements have been accomplished in this field over the past decade.[25–37] However, no efforts were put on the construction of chiral silica, although many biomimetic silicas were deposited by co-precipitation with chiral polypeptides.[25–28]

Among biomimetic silica formation, the silicateins particularly attracted our interest because they form axial filaments (fibrils) and act as templates to deposit silica around the surface of the fibrils to give fibrous hybrids consisted of axial filaments and silica shell.[20,22,23] Recently, we have established a novel silica-constructing program by mediation of soft nanocrystalline aggregates self-organized from linear polyethyleneimine (sPEI).[32] As the crystalline aggregates consist of a large amount of basic amine groups on their surface, they themself act as templates and catalysts promoting the hydrolysis of alkoxysilane and silica formation surrounding the templates to yield nanostructured powders or thin films with versatilely controlled shapes.[33–35] To build up structurally controlled chiral silica, we expanded our crystalline sPEI approach to a chiral crystalline complex (CCC) by association of sPEI with chiral tartaric acid and used the CCC as a catalytic template in chiral silica deposition.

As shown in Figure 1a, a very simple mixing process of adding an aqueous solution of tartaric acid to a hot aqueous solution of sPEI with equimolar NH and COOH groups and then cooling the mixture could afford white solid species, denoted as complexes sPEI/T@D, sPEI/T@L, and sPEI/T@DL. As seen in XRD patterns (Figure 1b), the three precipitated complexes are crystalline. The two complexes possessing chirality from D or L-tartaric acid are slightly different to the counterpart containing the racemic DL moiety; in the range $2\theta = 23$–$25°$, the chiral complexes have double peaks, while the racemic complex appeared as a single peak, clearly indicating that the chiral sPEI/T@D, sPEI/T@L have a different structure compared to the racemic sPEI/T@DL. By means of $^{1}H$ and $^{13}C$ NMR and FTIR spectroscopy, TG-DTA, and elemental analysis (Supporting Informa-

[*] Prof. Dr. R.-H. Jin
Synthetic Chemistry Lab., Kawamura Institute of Chemical Research
631 Sakado, Sakura, 285-0078 (Japan)
and
Department of Material and Life Chemistry, Kanagawa University
and JST-CREST
3-27-1, Rokkakubashi, Kanagawa-ku, Yokohama-shi
Kanagawa-ken, 221-8686 (Japan)
E-mail: rhjin@kanagawa-u.ac.jp
Dr. H. Matsukizono
Synthetic Chemistry Lab., Kawamura Institute of Chemical Research
631 Sakado, Sakura, 285-0078 (Japan)

[**] This work was partly supported by the Core Research for Evolutional Science and Technology (CREST) (Japan) Science and Technology Corporation (JST). We are grateful to Prof. Yashima at Nagoya University who allowed us to freely use DRCD spectroscopy.

Supporting information for this article is available on the WWW under http://dx.doi.org/10.1002/anie.201108914.

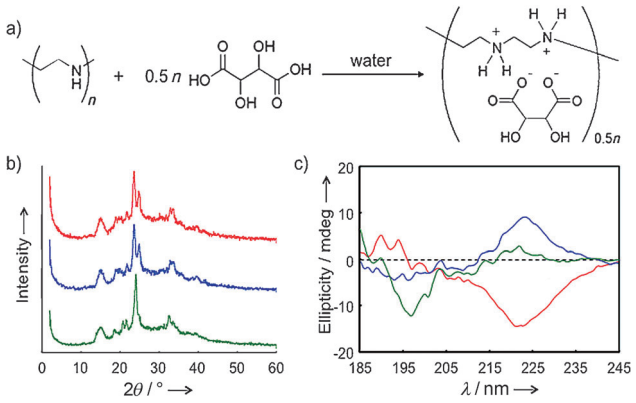


***Figure 1.*** Crystalline complexes formed from cooling the hot mixtures containing sPEI and D-, L-, or DL-tartaric acid. a) Representation of the formation of crystalline complexes, sPEI/T@D (red), sPEI/T@L (blue), and sPEI/T@DL (green). b) XRD patterns for three crystalline complexes. c) DRCD spectra for three crystalline complexes.

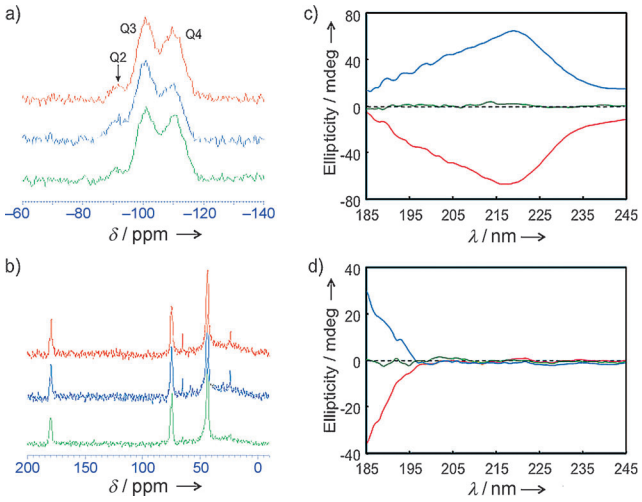


***Figure 2.*** The hybrids obtained by silica mineralization on the crystalline complexes. a) Solid-state $^{29}$Si MAS NMR spectra for three hybrids $SiO_2$/sPEI/T@D (red), $SiO_2$/sPEI/T@L (blue), and $SiO_2$/sPEI/T@DL (green). b) Solid-state $^{13}$C NMR spectra of the three hybrids. c), d) DRCD spectra of the silica materials $SiO_2$@L, $SiO_2$@D, and $SiO_2$@DL before (c) and after calcination (d).

tion, Figures S1–S4, Table S1), we confirmed the three complexes are composed of $CH_2CH_2NH$/tartrate/$H_2O$ 1:0.5:1.

These crystalline complexes were subjected to solid-state diffuse reflectance circular dichroism (DRCD). Interestingly, the sPEI/T@D and sPEI/T@L showed a negative and positive Cotton effect within their electronic absorption range 200–240 nm, respectively, which just appeared as a mirror pattern (Figure 1c) with opposite chiroptical signs against the powders of D- (positive) and L-tartaric acid (negative). As a matter of course, the racemic crystalline complex sPEI/T@DL was determined to be CD inactive. SEM showed that the chiral sPEI/T@D and sPEI/T@L appeared as roughly spherical aggregates with a twisted surface morphology, while the racemic sPEI/T@DL most likely consists of bundled sheets structures (Supporting Information, Figure S5), indicating the influence of enantiomeric purity of tartaric acid on the formation of morphologies of the crystalline complexes.

In the biomimetic silicification, polyamine is essential in silica deposition.[29,31,32] However, the synergistic effect from the association of amine groups with carboxyl groups is also able to actively promote silica mineralization.[36] Our polyamine/tartaric acid crystalline complexes are composed of amine- and carboxyl-terminated surface, which would satisfy the conditions to deposit silica. Employing sPEI/T@D, sPEI/T@L, and sPEI/T@DL as templates, we performed the silicification under neutral pH and ambient conditions by dispersing the crystalline complexes in a certain amount of water/TMOS (20:3 v/v) with stirring for 3 h. The resulting three solid products were subjected to solid-state $^{29}$Si MAS NMR, solid-state $^{13}$C NMR, XRD, TG-DTA, SEM, TEM, and DRCD. $^{29}$Si MAS NMR spectra (Figure 2a) revealed that the three solid products are silica that possess Q4 ($(SiO)_4Si$, $\delta = -110$ ppm) and Q3 ($(SiO)_3SiOH$, $\delta = -100$ ppm) as major bonding motifs, while $^{13}$C NMR spectra (Figure 2b) confirmed the presence of three carbon residues attributed to sPEI ($CH_2$-NH-$CH_2$, $\delta = 43$ ppm) and tartaric acid (HC-OH, $\delta = 75$ ppm, C=O, $\delta = 180$ ppm). These results distinctly imply that the three products are hybrids consisted of silica, sPEI, and tartaric acid (that is, $SiO_2$/sPEI/T@D, $SiO_2$/sPEI/T@L, and $SiO_2$/sPEI/T@DL). The content of the organic residues in these hybrids as estimated by TG-DTA was nearly 50 wt%. These organic components remained still somewhat crystalline in sPEI/T@D, sPEI/T@L, sPEI/T@DL, as seen in their characteristic XRD diffraction patterns (Supporting Information, Figure S6), indicating that in these hybrids, the crystalline complexes are included in the resulting silica. SEM images revealed that these hybrids are large aggregates agglomerated from micrometer-sized spherical particles (Supporting Information, Figure S7a). The surface of the chiral hybrids $SiO_2$/sPEI/T@D and $SiO_2$/sPEI/T@L showed a fiber-network structure, while the racemic hybrid $SiO_2$/sPEI/T@DL was structured by closely stacked nanosheets (Supporting Information, Figure S7b). Some crushed pieces from the spherical particulates were subjected to TEM observation, and we found that the chiral hybrids $SiO_2$/sPEI/T@D and $SiO_2$/sPEI/T@L have fibrous and very thin ribbon-like structures without any helical shape, while the racemic hybrid $SiO_2$/sPEI/T@DL appeared as stacked thick sheets (Supporting Information, Figure S7b).

The three hybrid particles were investigated by DRCD spectroscopy. In contrast to the racemic hybrid, which was inactive in DRCD spectrum in the wavelength range 200–300 nm, the chiral hybrid showed an intense CD signal: a negative ellipticity peak for $SiO_2$/sPEI/T@D and a positive ellipticity peak for $SiO_2$/sPEI/T@L, forming a mirror image around at 218 nm (Figure 2c). This chiroptical behavior is almost near to the chiral complexes sPEI/T@D and sPEI/T@L. To demonstrate whether the chiral structure is imprinted to the silica, we transformed both the chiral hybrids into the corresponding silica $SiO_2$@D and $SiO_2$@L by removing the organic components by calcination at 600 °C for 3 h. This calcination did not change the CD sign of the resultant $SiO_2$@D and $SiO_2$@L, and only caused the shift of the ellipticity peaks to shorter wavelength (180–190 nm), arising

  

from $SiO_2$ absorption (Figure 2d). It is surprising to find that the silica $SiO_2$@D calcined when the temperature was raised further (900 °C) still had a negative ellipticity peak (Supporting Information, Figure S8). Instead of the calcination, we selectively removed the residues of tartaric acid from the hybrid by treatment of the hybrid $SiO_2$/sPEI/T@D with 0.1 % $NH_3$ solution and found negative ellipticity peak from the residue particles (consisted of silica and sPEI, denoted as $SiO_2$/sPEI@D; Supporting Information, Figure S9). These results unambiguously reveal that the silica wall, once directed by CCC under neutral pH and room temperature silicification, is imprinted with chiral structure and the imprinted chiral silica wall is capable of maintaining its chirality even after treated at ultrahigh temperature. Such high thermoresistance is not observed in the case of chiral mesoporous silica, the helical chirality of which is instable against high-temperature calcination.[6,7] We performed a control experiment using non-crystalline complexes consisting branched polyethyleneimine (bPEI)/tartaric acid to deposit silica and found that the resulted silica with a chiral tartrate moiety did not resist calcination (for details, see the Supporting Information, Figure S10).

As a reliant examination of chirality, we introduced achiral chromophores onto the calcined chiral silica by chemical modification and physical adsorption, and investigated their induced CD spectra. The chromophore of $PhSiO_3$ chemically bound onto the 600 °C and 900 °C calcined $SiO_2$@D and $SiO_2$@L showed a induced DRCD spectra with perfect mirror pattern just within the UV absorbance band (210–280 nm) of the $PhSiO_3$ group (Figure 3a). It is worth noting that the silica powders, even when treated at 900 °C, are able to induce the CD activity of the achiral guest. Similar to the chemically bounded chromophore, a porphyrin residue physically adsorbed on the chiral silica (calcined at 600 °C) displayed induced DRCD spectra with formation of mirror relation at the Soret band (420–450 nm) of the porphyrin (Figure 3b). These induced DRCD spectra retained the same signs of ellipticity with the initial chiral silica $SiO_2$@L and $SiO_2$@D. Furthermore, we performed encapsulation of gold nanoparticles in the chiral silica by spontaneous in situ reduction[37] of $NaAuCl_3$ by mixing with the both chiral hybrids $SiO_2$/sPEI@D and $SiO_2$/sPEI@L in which the sPEI can reduce the ionic gold. Crystalline gold nanoparticles (Supporting Information, Figure S11) formed on $SiO_2$/sPEI@D and $SiO_2$/sPEI@L showed negative and positive ellipticity (Figure 3c), respectively, within the wavelength range around 450–700 nm that corresponds to nanoscale gold plasmon absorption (Figure 3d). This indicates the existence of considerable interactions between gold nanoparticles formed in situ and chiral silica wall, which led to the inductive chirality of the gold nanoparticles.

To investigate the influence of calcination temperature on the pore structure of chiral silica, we performed $N_2$ adsorption/desorption on the $SiO_2$@D calcined at different temperatures, such as 600, 700, 800, and 900 °C (Supporting Information, Figure S12) and found that the BET surface area (micropore area, external surface area) decreased with increasing the calcination temperature in the following order: 665 (553, 114) > 657 (553, 104) > 601 (491, 110) > 402 (317, 85) $m^2 g^{-1}$. In the case of the calcined chiral silica, obviously, the majority of the surface area was occupied by micropore area, which decreases suddenly at 900 °C calcination, while the external surface area is the minority and relatively stable. Considering together with the thermoresistant chirality, we are sure that ultrahigh temperature calcination can reduce the surface area with dramatically decreasing micropore frame of the silica but not destroy the geometrically ordered chiral structures on the silica wall.

In conclusion, the silica generated on chiral crystalline catalytic template has fibrous and very thin nanoribbon structures on which chirality is imprinted with silica formation. Compared to chiral mesoporous silica, which has helical-type chirality with a definite pitch, our chiral silica did not show a topologically characteristic helix. Thus we propose that in our chiral silica, geometrical chiral blocks with the same chiroptical signs are distributed randomly through the silica wall (Scheme 1). This randomly imprinted chirality would resist the high-temperature sintering with retention of the chiral performance and would be able to induce achiral guests, including molecules and nanoparticles, with chirality once the guests are simply bound onto the silica.

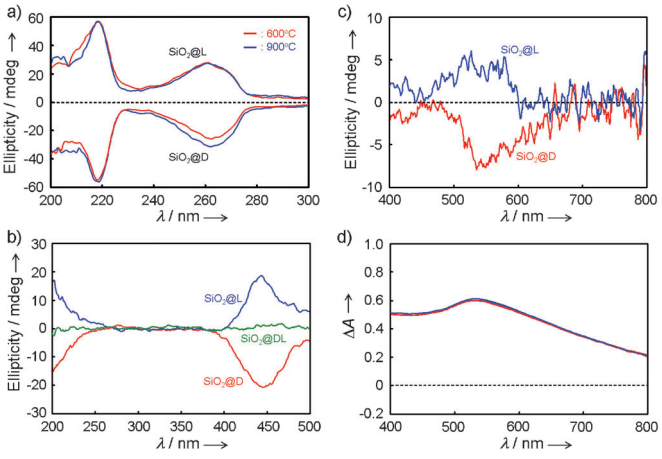


***Figure 3.*** Induced DRCD spectra on the chiral silica. a) After introduction of $PhSiO_3$ residues onto $SiO_2$@D and $SiO_2$@L calcined at 600 °C (red) and 900 °C (blue); b) after adsorption of tetrakis(3,5-hydroxyphenyl)porphyrin onto $SiO_2$@D and $SiO_2$@L and $SiO_2$@DL calcined at 600 °C; c) gold nanoparticles encapsulated by $SiO_2$/sPEI@D and $SiO_2$/sPEI@L; d) diffuse reflectance absorption spectra of gold nanoparticles on $SiO_2$/sPEI@D and $SiO_2$/sPEI@L.

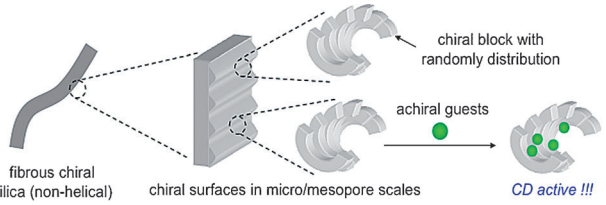


***Scheme 1.*** Representation of geometrically ordered chiral blocks distributed randomly through the silica wall and bounded chromophores.

## Experimental Section

Synthesis of chiral crystalline complex sPEI/T@D: sPEI (316 mg, 4.00 mmol for EI units) were dissolved in water (4 mL) at ca. 100 °C to afford sPEI solution ([EI] = 1000 mM). An aqueous solution (4 mL) of 500 mM of D-tartaric acid (300 mg, 2.00 mmol) was added slowly to the solution and the mixture was stirred for a few minutes at 100 °C. After the solution was cooled to room temperature, white precipitates were produced at an apparent pH for the water phase of 6.8. The precipitates were collected by suction filtration and washed with water. After drying at ambient atmosphere overnight, sPEI/T@D (477 mg, yield 88 %; white powder) was obtained.

Preparations of complexes of sPEI with other tartaric acids (sPEI/T@L, sPEI/T@DL) were performed by the same procedure mentioned above. sPEI/T@L: 485 mg (89 %), sPEI/T@DL: 499 mg (92 %).

Silica deposition on sPEI/T@D: The precipitates of crystalline complex sPEI/T@D formed from the mixture sPEI and D-tartaric acid ([EI] = 500 mM, [tartaric acid] = 250 mM) were washed three times with water by centrifugation (11180 × g) for 10 min at 20 °C and then dispersed in 23 mL of silica source solution (water/TMOS = 20/3 by vol.). The mixture was stirred vigorously for 3.5 h at room temperature and the solids were centrifuged and washed twice with 2-propanol to give a white solid, yield 416 mg ($SiO_2$/sPEI/T@D). The same method yielded $SiO_2$/sPEI/T@L (449 mg) and $SiO_2$/sPEI/T@DL (386 mg).

The values of weight loss in three hybrids were calculated to be 56, 56, and 63 %, respectively, for $SIO_2$/sPEI/T@D, $SiO_2$/sPEI/T@L, and $SiO_2$/sPEI/T@DL, from TG measurements. Calcination of these hybrids at definite temperatures (500–900 °C) resulted in the corresponding silica materials $SiO_2$@D, $SiO_2$@L, and $SiO_2$@DL. The introduction of a $PhSiO_3$ group was performed by stirring the mixture containing the powders of chiral silica calcined at 600 °C, phenytrimethoxysilane, and a solution of ethanol/28 % $NH_3$(aq) at room temperature for 24 h. The adsorption of the porphyrin was performed by mixing the chiral silica with the dichloromethane solutions of the chromophores for 3 h.

Received: December 18, 2011
Revised: March 13, 2012
Published online: April 26, 2012

**Keywords:** biomimetic silicification · chiral silica · chirality · crystalline templates · nanomaterials

[1] A. Guijarro, M. Yus, *The Origin of Chirality in the Molecules of Life*, RSC, Cambridge, **2009**.
[2] A. J. Gellman, *ACS Nano* **2010**, *4*, 5 – 10.
[3] R. E. Morris, X. Bu, *Nat. Chem.* **2010**, *2*, 353 – 361.
[4] S. Che, Z. Liu, T. Ohsuna, K. Sakamoto, O. Terasaki, T. Tatsumi, *Nature* **2004**, *429*, 281 – 284.
[5] H. Qiu, Y. Inoue, *Angew. Chem.* **2009**, *121*, 3115 – 3118; *Angew. Chem. Int. Ed.* **2009**, *48*, 3069 – 3072.
[6] S. Marx, D. Avnir, *Acc. Chem. Res.* **2007**, *40*, 768 – 776.
[7] S. Fireman-Shoresh, I. Popov, D. Avnir, S. Marx, *J. Am. Chem. Soc.* **2005**, *127*, 2650 – 2655.
[8] S. Fireman-Shoresh, S. Marx, D. Avnir, *Adv. Mater.* **2007**, *19*, 2145 – 2150.
[9] S. Lacasta, V. Sebastian, C. Casado, A. I. Mayoral, P. Romero, A. Larrea, E. Vispe, P. Lopez-Ram-de-Viu, S. Uriel, J. Coronas, *Chem. Mater.* **2011**, *23*, 1280 – 1287.
[10] *Silicon Biomineralization*: *Biology-Biochemistry-Molecular Biology-Biotechnology* (Ed.: W. E. G. Muller), Springer, Berlin, **2003**.
[11] F. E. Round, R. M. Crawford, D. G. Mann, The diatoms: biology & morphology of the genera., Cambridge University Press, **1999**.
[12] J. Aizenberg, J. C. Weaver, M. S. Thanawala, V. C. Sundar, D. E. Morse, P. Fratzl, *Science* **2005**, *309*, 275 – 278.
[13] J. C. Weaver, J. Aizenberg, G. E. Fantner, D. Kisailus, A. Woesz, P. Allen, K. Fields, M. J. Porter, F. W. Zok, P. K. Hansma, P. Fratzl, D. E. Morse, *J. Struct. Biol.* **2007**, *158*, 93 – 106.
[14] N. Kroger, R. Deutzmann, M. Sumper, *Science* **1999**, *286*, 1129 – 1132.
[15] N. Kroger, G. Lehmann, R. Rachel, M. Sumper, *Eur. J. Biochem.* **1997**, *250*, 99 – 105.
[16] N. Kroger, R. Deutzmann, C. Bergsdorf, M. Sumper, *Proc. Natl. Acad. Sci. USA* **2000**, *97*, 14133 – 14138.
[17] N. Poulsen, M. Sumper, N. Kroger, *Proc. Natl. Acad. Sci. USA* **2003**, *100*, 12075 – 12080.
[18] M. Sumper, E. Brunner, *ChemBioChem* **2008**, *9*, 1187 – 1194.
[19] K. Shimizu, J. N. Cha, G. D. Stucky, D. E. Morse, *Proc. Natl. Acad. Sci. USA* **1998**, *95*, 6234 – 6238.
[20] J. N. Cha, K. Shimizu, Y. Zhou, S. C. Christiansen, B. F. Chmelka, G. D. Stucky, D. E. Morse, *Proc. Natl. Acad. Sci. USA* **1999**, *96*, 361 – 365.
[21] W. E. G. Müller, C. Eckert, K. Kropf, X. Wang, U. Schloßmacher, C. Seckert, S. E. Wolf, W. Tremel, H. C. Schröder, *Cell Tissue Res.* **2007**, *329*, 363 – 378.
[22] W. E. G. Müller, X. Wang, F.-Z. Cui, K. P. Jochum, W. Tremel, J. Bill, H. C. Schröder, F. Natalio, U. Schloßmacher, M. Wiens, *Appl Microbiol. Biotechnol.* **2009**, *83*, 397 – 413.
[23] E. Mugnaioli, F. Natalio, U. Schloßmacher, X. Wang, W. E. G. Müller, U. Kolb, *ChemBioChem* **2009**, *10*, 683 – 689.
[24] H. C. Schröder, D. Brandt, U. Schloßmacher, X. Wang, M. N. Tahir, W. Tremel, S. I. Belikov, W. E. G. Müller, *Naturwissenschaften* **2007**, *94*, 339 – 359.
[25] J. N. Cha, G. D. Stucky, D. E. Morse, T. J. Deming, *Nature* **2000**, *403*, 289 – 292.
[26] F. Rodríguez, D. D. Glawe, R. R. Naik, K. P. Hallinan, M. O. Stone, *Biomacromolecules* **2004**, *5*, 261 – 265.
[27] M. M. Tomczak, D. D. Glawe, L. F. Drummy, C. G. Lawrence, M. O. Stone, C. C. Perry, D. J. Pochan, T. J. Deming, R. R. Naik, *J. Am. Chem. Soc.* **2005**, *127*, 12577 – 12582.
[28] V. M. Yuwono, J. D. Hartgerink, *Langmuir* **2007**, *23*, 5033 – 5038.
[29] K. M. Roth, Y. Zhou, W. Yang, D. E. Morse, *J. Am. Chem. Soc.* **2005**, *127*, 325 – 330.
[30] A. Bernecker, R. Wieneke, R. Riedel, M. Seibt, A. Geyer, C. Steinem, *J. Am. Chem. Soc.* **2010**, *132*, 1023 – 1031.
[31] S. V. Patwardhan, *Chem. Commun.* **2011**, *47*, 7567 – 7582.
[32] R.-H. Jin, J.-J. Yuan, *Chem. Commun.* **2005**, 1399 – 1401.
[33] J.-J. Yuan, R.-H. Jin, *Adv. Mater.* **2005**, *17*, 885 – 888.
[34] R.-H. Jin, J.-J. Yuan, *Adv. Mater.* **2009**, *21*, 3750 – 3753.
[35] H. Matsukizono, R.-H. Jin, *Langmuir* **2011**, *27*, 6338 – 6348.
[36] A. F. Wallace, J. J. DeYoreo, P. M. Dove, *J. Am. Chem. Soc.* **2009**, *131*, 5244 – 5250.
[37] J.-J. Yuan, P.-X. Zhu, N. Fukazawa, R.-H. Jin, *Adv. Funct. Mater.* **2006**, *16*, 2205 – 2212.

  